

# INTRINSIC LOCALIZED MODES IN PERIODIC NONLINEAR LATTICES UNDER SIMULTANEOUS EXCITATIONS

Diala Bitar, Najib Kacem and Nouredine Bouhaddi

*Univ. Bourgogne Franche-Comté, FEMTO-ST Institute, CNRS/UFC/ENSMM/UTBM,  
Department of Applied Mechanics, 25000 Besançon, France  
email: diala.bitar@femto-st.fr*

Intrinsic Localized Modes (ILMs) or solitons are investigated in periodic arrays of coupled nonlinear resonators under simultaneous external and parametric excitations. The method of multiple scales is employed, transforming the dimensionless equations of motion into a damped driven Nonlinear Schrödinger (NLS) equation. Exact stationary soliton solutions of the undamped driven NLS equation are derived, while the damped one is numerically solved using the continuous analog of the Newton method. Several numerical simulations have been performed in order to investigate the evolution of the existence and stability domains of soliton solutions with respect to the linear damping and the excitation type. In practice, this approach can be used to design nonlinear periodic lattices enabling the creation of stabilized solitons for energy transport applications.

**Keywords:** Intrinsic localized modes, nonlinear lattices, simultaneous excitations, Schrödinger equation

---

## 1. Introduction

In the theory of waves in nonlinear periodic structures, spatial localization is one of the most important properties encountered in nonlinear normal modes, providing a link between these modes and solitary solutions. It can be generated either by an extrinsically imposed disorder as in the case of the Anderson localization or by the interaction between the inherent nonlinearities of the resonators. The localization represents an interesting phenomenon in engineering science, which can occur in periodic structures when the wave-function amplitude of the oscillating modal shape is localized in space and decays exponentially. This phenomenon has inspired innovative studies in physics and motivated researchers over many years to explore in depth its effects and consequences. Voluminous studies on mode localization in discrete and continuous periodic nonlinear systems exist in engineering physics using appropriate analytical and numerical techniques. ILMs have been observed in Josephson junctions coupled arrays [1], antiferromagnet [2], optics [3], photonics [4], carbon nanotubes [5, 6, 7] and atomic lattices [8]. ILMs received a lot of attention in micromechanical resonators arrays [9], Kenig et al. [10] studied the ILMs in arrays of parametrically driven nonlinear oscillators with application to MEMS and NEMS systems. For granular crystals chains, it has been shown that the interplay of periodicity, nonlinearity driving and asymmetry allows the exploration of localization phenomena including solitons and Discrete Breathers (DBs) [11].

Several analytical and numerical studies were devoted to solve parametrically and externally driven damped NLS equations [12, 13]. The richness of the nonlinear dynamics in terms of stability and multivaluedness responses obtained in weakly coupled nonlinear oscillators under both external [14] and simultaneous primary and parametric excitations [15], motivated the study of ILMs

in simultaneously driven nonlinear arrays. Recently, the influence of adding external harmonic excitation on the intrinsic localized modes of coupled pendulums chains parametrically excited has been investigated [16]. A perturbation technique is employed, transforming the coupled nonlinear equations of motion of the periodic array into a damped, simultaneously driven NLS equation. Exact stationary solutions of the conservative NLS equation are derived, while the dissipative system is numerically solved using the continuous analog Newton method. Several numerical simulations have been performed in order to highlight the additional value of employing both external and parametric excitations simultaneously on the stability of localized solutions.

## 2. Derivation of the amplitude equation

The normalized equations of motion (EoMs) of an array of coupled Duffing oscillators, under simultaneous external and parametric excitation can be written in the following form

$$\ddot{u}_n - \frac{1}{2}\varepsilon^{1/2}D(u_{n+1} - 2u_n + u_{n-1}) + \varepsilon\hat{\gamma}\dot{u}_n + u_n + \varepsilon\hat{h}\cos[2(1 + \varepsilon\Omega)t]u_n + \hat{\delta}[(u_n - u_{n+1})^3 + (u_n - u_{n-1})^3] + \hat{\xi}u_n^3 = \varepsilon^{3/2}\hat{g}\cos[(1 + \varepsilon\Omega)t] \quad (1)$$

As the resonators are collectively oscillating at almost the same frequency, we write the displacement of the  $n^{\text{th}}$  resonator as [10]:

$$u_n = \varepsilon^{1/2}[\hat{\psi}(\hat{X}_n, \hat{T})e^{i(t-\pi n)} + c.c.] + \varepsilon^{3/2}u_n^{(1)}(t, \hat{T}, \hat{X}_n) + \dots \quad n = 1, \dots, N, \quad (2)$$

with  $c.c.$  representing the complex conjugate,  $T = \varepsilon t$  and  $\hat{X}_n = \varepsilon^{1/4}n$  are slow temporal and spatial variables. Writing the continuous variable  $\hat{X}$  in place of  $\hat{X}_n$  and replacing the displacement solution (2) into the normalized equation of motion term by term up to order  $\varepsilon^{3/2}$  we obtain:

$$\dot{u}_n = \varepsilon^{1/2}\left[\left(\varepsilon\frac{\partial\hat{\psi}}{\partial\hat{T}} + i\hat{\psi}\right)e^{i(t-\pi n)} + c.c.\right] + \varepsilon^{3/2}\dot{u}_n^{(1)} \quad (3)$$

$$\ddot{u}_n = \varepsilon^{1/2}\left[\left(\varepsilon^2\frac{\partial^2\hat{\psi}}{\partial\hat{T}^2} + 2i\varepsilon\frac{\partial\hat{\psi}}{\partial\hat{T}} - \hat{\psi}\right)e^{i(t-\pi n)} + c.c.\right] + \varepsilon^{3/2}\ddot{u}_n^{(1)} \quad (4)$$

$$u_n^3 = 3\varepsilon^{3/2}|\hat{\psi}|^2\hat{\psi}e^{i(t-\pi n)} + O(e^{3it}, e^{3i\pi n}) + c.c. \quad (5)$$

$$u_{n\pm 1} = -\varepsilon^{1/2}\left[\left(\hat{\psi} \pm \varepsilon^{1/4}\frac{\partial\hat{\psi}}{\partial\hat{X}} + \frac{\varepsilon^{1/2}}{2}\frac{\partial^2\hat{\psi}}{\partial\hat{X}^2}\right)e^{i(t-\pi n)} + c.c.\right] + \varepsilon^{3/2}u_{n\pm 1}^{(1)} \quad (6)$$

$$u_{n+1} - u_n + u_{n-1} = -\varepsilon^{3/2}\frac{\partial^2\hat{\psi}}{\partial\hat{X}^2}e^{i(t-\pi n)} + c.c. \quad (7)$$

$$[(u_n - u_{n+1})^3 + (u_n - u_{n-1})^3] = \varepsilon^{3/2}48|\hat{\psi}|^2\hat{\psi}e^{i(t-\pi n)} + O(e^{3it}, e^{3i\pi n}) + c.c. \quad (8)$$

$$\varepsilon\cos[2(1 + \varepsilon\Omega)t]u_n = \frac{1}{2}\varepsilon^{3/2}\hat{\psi}^*e^{i\Omega\hat{T}}e^{i(t+\pi n)} + O(e^{3it}) + c.c. \quad (9)$$

$$\cos[(1 + \varepsilon\Omega)t] = -\frac{1}{2}\varepsilon^{1/2}e^{i\frac{\Omega}{2}\hat{T}}e^{i(t-\pi n)} + c.c. \quad (10)$$

where  $O(e^{3it}, e^{3i\pi n})$  are rapidly oscillating terms with 3 and  $3\pi$  as the temporal frequency and the spatial wave number respectively. Although, the EoMs (1) are trivially satisfied at the order  $\varepsilon^{1/2}$ , one must satisfy a solvability condition at the order  $\varepsilon^{3/2}$  by vanishing all terms proportional to  $e^{i(t-\pi n)}$  so that  $u_n^{(1)}$  remains finite. Then, we obtain the following partial differential equation (PDE) defining the slow dynamics of the resonators amplitudes

$$2i\frac{\partial\hat{\psi}}{\partial\hat{T}} + (48\hat{\delta} + 3\hat{\xi})|\hat{\psi}|^2\hat{\psi} + \frac{1}{2}D\frac{\partial^2\hat{\psi}}{\partial\hat{X}^2} + i\hat{\gamma}\hat{\psi} - \frac{\hat{h}}{2}\hat{\psi}^*e^{2i\Omega\hat{T}} = -\frac{\hat{g}}{2}e^{i\Omega\hat{T}} \quad (11)$$

Using the following scaling parameters

$$\hat{\psi} = \sqrt{\frac{2\Omega}{48\hat{\delta} + 3\hat{\xi}}} \psi, \quad X = \sqrt{\frac{D}{2\Omega}} X, \quad \hat{T} = \frac{2}{\Omega} T, \quad \hat{\gamma} = \Omega\gamma, \quad \hat{h} = 2\Omega h, \quad \hat{g} = 2\Omega \sqrt{\frac{2\Omega}{48\hat{\delta} + 3\hat{\xi}}} g,$$

Eq. (11) can be transformed into an autonomous normalized PDE after replacing  $\psi$  by  $\psi e^{iT}$  as

$$i\frac{\partial\psi}{\partial T} = -\frac{\partial^2\psi}{\partial X^2} + (1 - i\gamma)\psi - 2|\psi|^2\psi + h\psi^* - g \quad (12)$$

Eq. (12) describes a nonlinear time dependent Schrödinger equation, including both external and parametric driving forces beside the linear damping parameter. With  $\gamma = 0$  and  $\gamma \neq 0$  Eq. (12) is called Conservative or Dissipative Simultaneously Driven NonLinear Schrödinger equations (CSDNLS) or (DSDNLS) respectively.

## 2.1 Exact analytical solitary solutions of the CSDNLS equation

As a first step, searching for the ground state which has the form of a localized (in space) exact solutions. Given a real solution  $\psi(x, t)$  for the following CSDNLS equation ( $\gamma = 0$ ):

$$i\psi_T + \psi_{XX} - H\psi + 2\psi|\psi|^2 = -g, \quad (13)$$

with  $H = (1 + h)$ . Each  $\tilde{\psi}(X, T) = k\psi(kX, k^2T)$  is also a solution, corresponding to  $\tilde{g} = k^3g$  and  $\tilde{H} = k^2H$ . Consequently, any solution to Eq. (13) is characterized, up to a simple scaling, by a single combination  $f = gH^{-3/2}$  as given by Barashenkov et al. [13]. In addition, they found two different soliton solutions of Eq. (13) of the form:

$$\psi_{\pm}(X) = \psi_0 \left( 1 + \frac{2 \sinh^2 \alpha}{1 \pm \cosh \alpha \cosh(AX)} \right), \quad (14)$$

Where  $f$  is the monotonously decreasing function of  $h$  and  $g$  defined as [16]:

$$f = \frac{g}{(1 + h)^{3/2}} = \frac{\sqrt{2} \cosh^2 \alpha}{(1 + 2 \cosh^2 \alpha)^{3/2}}. \quad (15)$$

$f$  being a monotonically decreasing function,  $\alpha$  is uniquely determined by  $h$  and  $g$ .  $\psi_0$  is the asymptotic value of both  $\psi_-$  and  $\psi_+$  solitons:  $\psi_{\pm}(X) \rightarrow \psi_0$  as  $|X| \rightarrow \infty$

Finally,  $A$  has the meaning of "half the area" of both solitons  $\psi_-$  and  $\psi_+$  and is equal to  $A = 2\psi_0 \sinh \alpha = \frac{1}{2} \int (\psi_{\pm}(X)^2 - \psi_0^2) dX$

$$\psi_0 \text{ is real and positive: } \psi_0 = \frac{1}{\sqrt{2(1 + 2 \cosh^2 \alpha)}} = \left( \frac{g}{4(1 + h)^{3/2} \cosh^2 \alpha} \right)^{1/3} \quad (16)$$

We should note that these solutions exist for  $\alpha \in [0, \infty]$  or for  $f = \frac{g}{(1 + h)^{3/2}} \in [0, \sqrt{2/27}]$  in terms of excitations amplitudes. Fig. 1 (left) shows the domain of existence of  $\alpha$  according to the different values of the driving forces  $h$  and  $g$ . Fig. 1 (right) shows the evolution of the solitary solutions  $\psi_{\pm}$  of the CSDNLS equation according to  $\alpha$ .

## 2.2 Numerical solutions of the DSDNLS equation

For positive linear damping coefficient ( $\gamma > 0$ ), Eq. (12) is solved numerically using the continuous analog of the Newton method (also known by the variable iteration step Newton method).

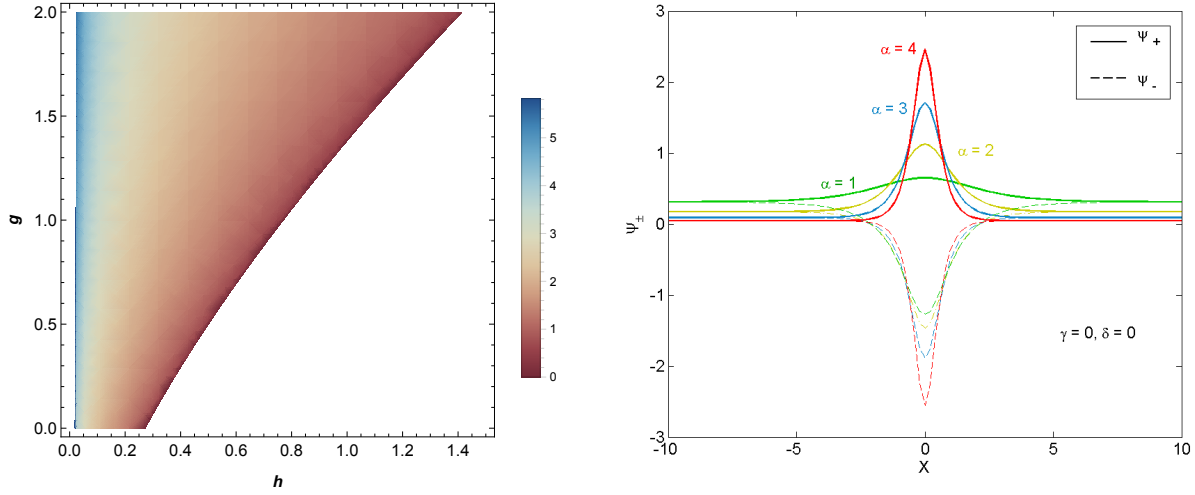


Figure 1: Left curve defines the existence domain of  $\alpha$  according to the driving forces  $h$  and  $g$ . The right curve shows the undamped solitary solutions  $\psi_{\pm}$  of the SDNLS equation for several values of  $\alpha$ .

To solve the PDE (12) numerically, we write it on its finite difference form on the discretized domain  $[-L/2, L/2]$  as  $\mathbf{E}(\psi) = 0$  with  $\psi = (\psi_1, \psi_2, \dots, \psi_{N+1})$  discretized solution, with  $\psi_n = \psi(X_n)$ ,  $X_n = -\frac{L}{2} + n\Delta X$ ,  $\Delta X = \frac{L}{N+1}$  and  $\mathbf{E} = (E_1, E_2, \dots, E_{N+1})$  is a nonlinear operator defined as follows

$$E_n = \frac{\psi_{n+1} - 2\psi_n + \psi_{n-1}}{(\Delta X)^2} - \psi_n + 2|\psi_n|^2\psi_n + i\gamma\psi_n - h\psi_n^* + g; \quad \text{for } n = 1 \dots N \quad (17)$$

$$\text{with } E_0 = \frac{-3\psi_0 + 4\psi_1 - \psi_2}{2\Delta X} \quad \text{and} \quad E_{N+1} = \frac{\psi_{N-1} - 4\psi_N + 3\psi_{N+1}}{2\Delta X}. \quad (18)$$

This can be obtained using the finite difference approximations for both differential operators  $\psi_{XX}$  and  $\psi_X$  and satisfying the boundary conditions  $\psi_X(\pm L/2) = 0$ . The basic concept of the continuous analog Newton's method is to introduce an additional growing variable  $\tau$ , in such a manner that  $\psi$  satisfies the following differential equation  $\frac{d}{d\tau}\mathbf{E}(\psi(\tau)) + \mathbf{E}(\psi(\tau)) = 0$  with the initial conditions  $\psi(0) = \psi^{(0)}$  where  $\psi^{(0)}$  is considered to be the exact solitary solution of the SDNLS equation with no damping. As  $\mathbf{E}(\psi(\tau)) \xrightarrow{\tau \rightarrow +\infty} 0$ ,  $\psi(\infty)$  satisfies  $\mathbf{E}(\psi) = 0$ ,

$$\psi^{(k+1)} = \psi^{(k)} - \Delta\tau^{(k+1)} \left( \frac{\partial \mathbf{E}}{\partial \psi} \right)_{\psi=\psi^{(k)}}^{-1} \mathbf{E}(\psi^{(k)}) \quad \text{where } k = 1, 2, \dots \quad (19)$$

$\Delta\tau^{(k+1)} = \tau^{(k+1)} - \tau^{(k)}$  is selected in order to minimize the following residual

$$\delta^{(k)} = \max_{1 \leq n \leq N} \{ |\text{Re}E_n(\psi^{(k)})|, |\text{Im}E_n(\psi^{(k)})| \} \quad (20)$$

In order to implement the variable iteration step Newton method, we start by choosing a pair  $(g, h)$  of parameters in the domain of existence  $[0, \sqrt{2/27}]$ . Eq. (15) is used to determine the unique  $\alpha$  for the chosen  $(g, h)$ , and we start our continuation using the exact solitary solutions (14) as an approximation for  $\gamma = 0.01$ . Then, we calculate the numerical solution (19) for the same  $g, h$  and  $\gamma = 0.01$  and keep advancing along the path until convergence is achieved and residual (20) is minimized. After, we chose the obtained numerical solution for  $\gamma = 0.1$  as an approximation for the  $(g, h)$  pair with  $\gamma = 0.02$ , and the process repeated until the Newtonian iterations ceased to converge.

These calculations were performed on the interval  $(-L/2, L/2)$ , where the soliton solutions decay slowly in space ( $\psi_{\pm}(\pm L/2) = 0$ ). Finally, for a given  $\Delta x$ , the obtained  $\psi$  is used as a boundary condition for  $T = 0$  to solve the DSDNLS Eq. (12) numerically, using a Runge-Kutta algorithm

while setting  $\psi_T = 0$ . Barashenkov et al. [13] constructed the existence and stability chart for the soliton solutions of the externally driven, damped NLS equation given in Fig. 2. They showed that,  $\psi_+$  solution is unstable for all forcing amplitude  $g$  and dissipation coefficient  $\gamma$ . In Fig. 2, blue color indicates the stability region of  $\psi_-$ , while in the pink region  $\psi_-$  exists and it is unstable.

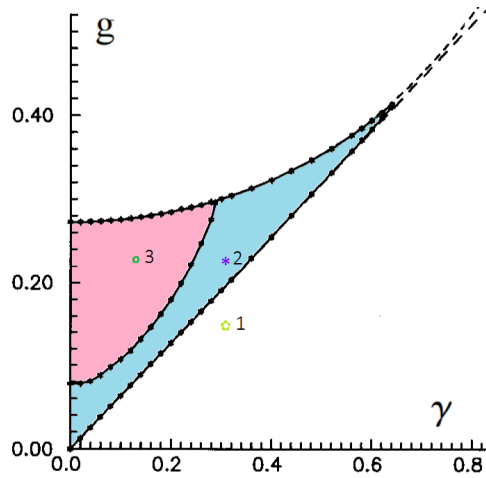


Figure 2: Existence and stability diagram for the soliton solutions of the externally driven damped NLS equation as constructed by Barashenkov et al. [13] on the plane of both forcing amplitude  $g$  and dissipation coefficient  $\gamma$ . They showed that,  $\psi_+$  soliton solution is unstable for all forcing amplitude  $g$  and dissipation coefficient  $\gamma$ . Blue color indicates the region where  $\psi_-$  exists and stable, while in the pink color represents the region where  $\psi_-$  exist but unstable.

### 3. Numerical simulations and interpretations

In this section we are interested in solving numerically the DSDNLS Eq. (12) for several sets of parameters. According to the existence and stability diagram (2) of the externally driven, damped NLS equation constructed by Barashenkov et al [13], the lower straight line defines an approximation for the lower boundary of the domain of existence of  $\psi_{\pm}$  solutions. For the pair of parameters ( $\star$  1) where the damping parameter is  $\gamma = 0.3$  and  $g = 0.232$ ,  $\psi_{\pm}$  are unstable. Particularly,  $\psi_+$  does not exist while  $\psi_-$  exists but decay to zero over time. Remarkably, adding a parametric excitation  $h = 0.15$ , Fig. 3 shows that both solitary solutions exist and converge for the same stable solution.

Now choosing the pair of parameters ( $\star$  2) in the blue region of Fig. 2. For these parameters and for  $h = 0$ ,  $\psi_+$  does not exist while  $\psi_-$  is stable. In contrast, when adding a parametric excitation  $h = 0.25$ , both localized solutions  $\psi_{\pm}$  exist as unexpected interesting results are revealed. Firstly, Fig. 4 shows that  $\psi_-$  loses its stability and oscillates periodically in time, as shown in the temporal solution and phase portrait curves (a) and (b). In addition, Figure 5 (a) shows that the initial transient gives rise to the formation of three solitons  $\psi_+$ , where the middle one decays to 0 and the two others are not perfectly and periodically stable. Barashenkov et al. [13] demonstrated that the stability of solitary solutions is very sensitive to the interval length. Therefore, increasing  $L$  to 100 which corresponds to  $N = 501$  dofs, Fig. 5 (b) shows the localized soliton solution  $\psi_+$ . Noteworthy the number of solitons increases up to 6 and they are periodically stable at  $T = 200$ . Note that before reaching the steady state, several pairs of solitons emerge into one.

The last configuration in Fig. 2 corresponds to the third pair of parameters ( $\circ$  4) in the pink region where  $\psi_+$  does not exist and  $\psi_-$  is unstable and represents a spatio-temporal chaos as shown in the left curve in Fig. 6 for  $h = 0$ . The right curve shows the evolution of  $|\psi_-|^2$  while adding a parametric excitation  $h = 0.225$ , which enables to avoid the collapse of spatiotemporal chaos.

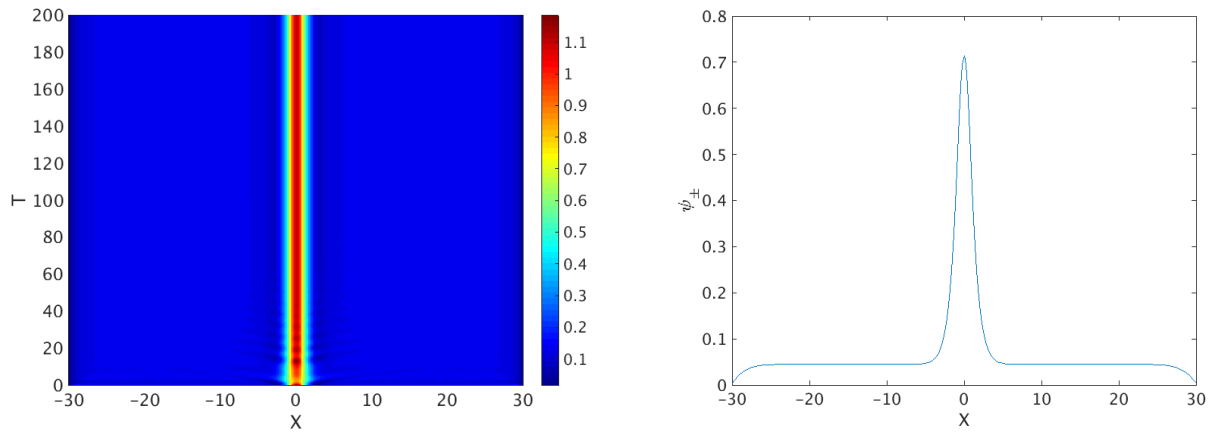


Figure 3: Left curve shows the evolution of  $|\psi_{\pm}|^2$  over time, while the left one shows the stable solution at  $T = 200$  for the first pair of parameters (★ 1) with  $\gamma = 0.3$ ,  $g = 0.15$ ,  $h = 0.15$  and  $L = 60$ .

## 4. Conclusion

We investigated the intrinsic localization in a one dimensional array of coupled Duffing oscillators under simultaneous parametric and external excitations. The multiple scales method was employed, transforming the differential system into an amplitude shrödinger equation, describing the spatio-temporal dynamics of the system. For zero dissipation, the analytical soliton solutions of the simultaneously driven NLS equation were determined. The DSDNLS equation was numerically solved as a boundary value problem over an interval of length  $L$ , using the continuous analog Newton's method.

Several simulations on different pairs of parameters were performed, based on the existence and stability domain of the externally driven, damped NLS equation. It has been shown that adding an amount of parametric driving force avoid spatiotemporel chaos and extend the stability domain according to the linear damping. Therefore, the combination between parametric and the external excitations, helps tuning the existence and stability of solitons solutions.

In practice, and since the damping parameter is often imposed by the system, this study can serve as a predicting numerical tool; allowing the control of the existence and stability of localized solutions by the simultaneous driving forces to localize energy or avoid energy localization.

## Acknowledgment

This project has been performed in cooperation with the Labex ACTION program (contract ANR-11-LABX-01-01).

## REFERENCES

1. Binder, P., Abraimov, D., Ustinov, A. V., Flach, S. and Zolotaryuk, Y., Observation of breathers in Josephson ladders, *Phys. Rev. Lett.*, **84**, 745–748, (2000).
2. Sato M. and Sievers, A. J., Direct observation of the discrete character of intrinsic localized modes in an antiferromagnet, *Nature*, **432**, 486–0836, (2004).
3. Sukhorukov, A. A., Kivshar, Y. S., Eisenberg, H. S. and Silberberg, Y., Spatial optical solitons in waveguide arrays, *IEEE J. Quant. Electron.*, **39** (1), 31–50, (2003).
4. Christodoulides, D. N., Lederer, F. and Silberberg, Y., Discretizing light behaviour in linear and nonlinear waveguide lattices, *Nature*, **424** (6950), 817–823, (2004).



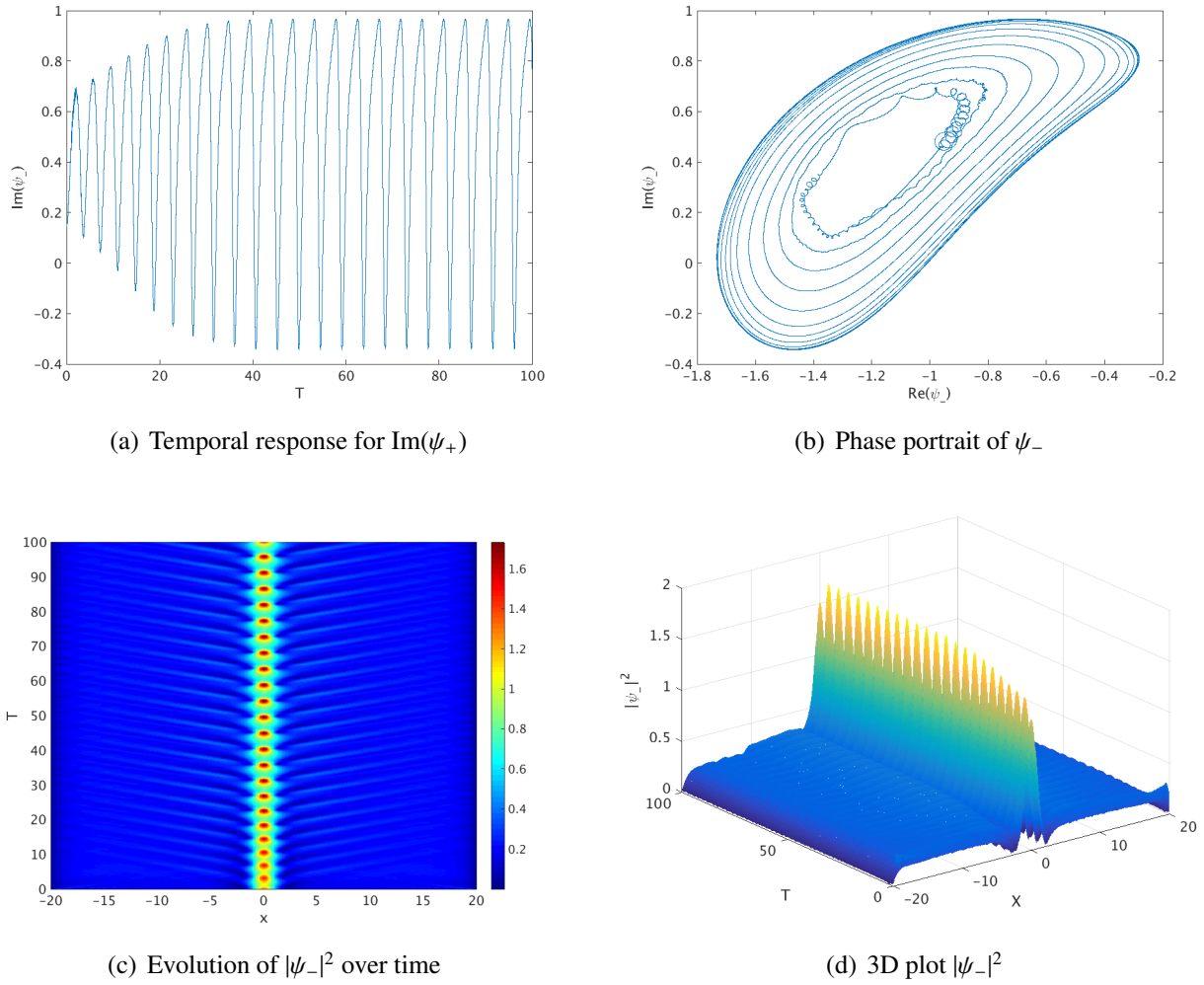


Figure 4: Evolution of  $|\psi_-|^2$  over time for (\*) 2) with  $\gamma = 0.3$ ,  $g = 0.232$ ,  $h = 0.25$  and  $L = 40$ .

5. Strozzi, M., Smirnov, V.V., Manevitch, L. I., Milani, M. and Pellicano, F., Nonlinear vibrations and energy exchange of single-walled carbon nanotubes. Circumferential flexural modes, *Journal of Sound and Vibration*, **381**, 156–178, (2016).
6. Smirnov, V. V., Shepelev, D. S. and Manevitch, L. I., Localization of bending vibrations in the single-walled carbon nanotubes, *Nanosystems: Physics, Chemistry, Mathematics*, **2** (2), 102–106, (2011).
7. Smirnov, V. V., Manevitch, L. I., Strozzi, M. and Pellicano, F., Nonlinear optical vibrations of single walled carbon nanotubes, *Physica D*, **325**, 113–125, (2016).
8. Bickham, S. R., Kiselev, S. A. and Sievers, A. J., Stationary and moving intrinsic localized modes in one-dimensional monatomic lattices with cubic and quartic anharmonicity, *Phys. Rev. B*, **47**, 14206–14211, (1993).
9. Sato, M., Hubbard, B. E., English, L. Q., Sievers, A. J., Ilic, B., Czapski, D. A. and Craighead, H. G., Study of intrinsic localized vibrational modes in micromechanical oscillator arrays, *Chaos*, **13** (2), 702–715, (2003).
10. Kenig, E., Malomed, B. A., Cross, M. C., and Lifshitz, R., Intrinsic localized modes in parametrically driven arrays of nonlinear resonators, *Phys. Rev. E*, **80**, 046202, (2009).
11. Chong, C., Kevrekidis, P. G., Theocharis, G. and Daraio, C., Dark breathers in granular crystals, *Phys. Rev. E*, **87**, 042202, (2013).

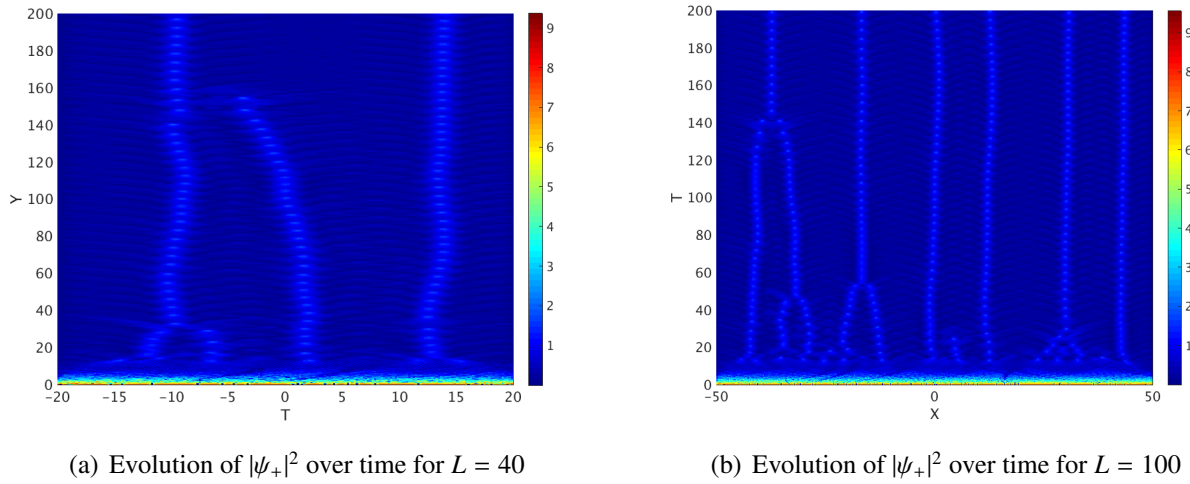


Figure 5: Evolution of  $|\psi_+|^2$  over time for the pair of parameters (\* 2)  $\gamma = 0.3$ ,  $g = 0.232$ ,  $h = 0.25$ .

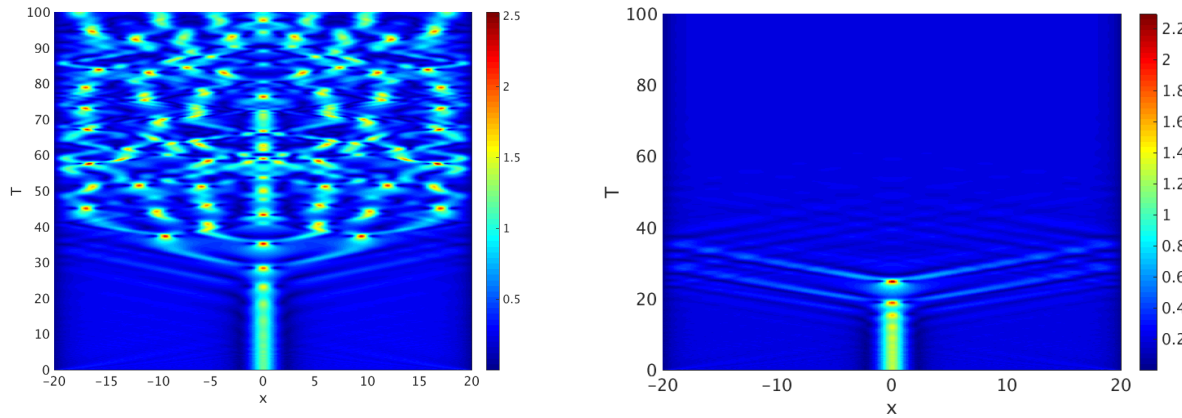


Figure 6: Evolution of  $|\psi_+|^2$  solution over time for the pair of parameters (◊ 3)  $\gamma = 0.1$ ,  $g = 0.232$   $L = 40$  with  $h = 0$  (Left curve) and  $h = 0.225$  (Right curve).

12. Barashenkov, I. V., Bogdan, M. M. and Korobov, V. I., Stability diagram of the phase-locked solitons in the parametrically driven, damped nonlinear schrödinger equation, *EPL*, **15** (2), 113–118, (1991).
13. Barashenkov, I. V. and Smirnov, Y. S., Existence and stability chart for the ac-driven, damped nonlinear schrödinger solitons, *Phys. Rev. E*, **54** (5), 5707–5725, (1996).
14. Bitar, D., Kacem, N. and Bouhaddi, N., Investigation of modal interactions and their effects on the nonlinear dynamics of a periodic coupled pendulums chain, *Int. J. Mech. Sci.* (In press, accepted manuscript on 30 Nov 2016). DOI: 10.1016/j.ijmecsci.2016.11.030.
15. Bitar, D., Kacem, N., Bouhaddi, N. and Collet, M., Collective dynamics of periodic nonlinear oscillators under simultaneous parametric and external excitations, *Nonlinear Dynamics*, **82** (1), 749–766, (2015).
16. Jallouli, A., Kacem, N. and Bouhaddi, N, Stabilization of solitons in coupled nonlinear pendulums with simultaneous external and parametric excitations, *Commun. Nonlinear Sci. Numer. Simul.*, **42** (1), 1–11, (2017).